

<sup>447</sup> **Chapter 5**

<sup>448</sup> **Synthesis**

<sup>449</sup> Improving decadal to centennial projections of global sea level rise is of utmost im-  
<sup>450</sup> portance for mitigating future environment and socio-economic impacts (Durand  
<sup>451</sup> et al., 2022). Antarctica's projected contributions to global sea level rise by the  
<sup>452</sup> end of the century under a high-emission scenario is between 0.03 and 0.28 m (RCP  
<sup>453</sup> 8.5, Intergovernmental Panel on Climate Change (IPCC), 2022). This wide range  
<sup>454</sup> of possible values expresses the uncertainty of the Antarctic Ice Sheet's response to  
<sup>455</sup> a warming world. Over 80% of ice loss from Antarctica occurs through ice shelves  
<sup>456</sup> (Rignot et al., 2013), highlighting their importance in reducing the uncertainty in  
<sup>457</sup> sea level rise projections. Antarctica's largest ice shelf, the Ross Ice Shelf, is fed  
<sup>458</sup> from both the East and West Antarctic Ice Sheets. Its catchment contains a total  
<sup>459</sup> volume of ice equivalent to 11.6 m of global sea level rise (Tinto et al., 2019; Fretwell  
<sup>460</sup> et al., 2013; Rignot et al., 2011). While the Ross Ice Shelf is relatively stable cur-  
<sup>461</sup> rently (Rignot et al., 2013; Moholdt et al., 2014), geologic evidence shows the rapid  
<sup>462</sup> destabilization of the ice shelf within the past ~7,000 years (e.g., Venturelli et al.,  
<sup>463</sup> 2020; Naish et al., 2009).

<sup>464</sup>

<sup>465</sup> The destabilization of the ice shelf is thought to have been primarily caused by  
<sup>466</sup> ocean forcings (Lowry et al., 2019), as bathymetric troughs guide in the inflow of  
<sup>467</sup> melt-inducing ocean circulations (Tinto et al., 2019). The subsequent grounding  
<sup>468</sup> line retreat however is predominantly controlled by the physiography and geology  
<sup>469</sup> of the region (Halberstadt et al., 2016). This highlights the solid earth, through its  
<sup>470</sup> bathymetric control on basal melt and its effects on grounding line retreat dynam-  
<sup>471</sup> ics, as an important component of the dynamics of the Ross Ice Shelf. To reliably  
<sup>472</sup> understand the contribution of the Ross Ice Shelf to future sea level rise, we must  
<sup>473</sup> provide ocean and ice modellers with the necessary geologic boundary conditions.  
<sup>474</sup> This thesis aimed to provide both these boundary conditions and estimates of their  
<sup>475</sup> uncertainties to the modelling community. A series of research questions were pro-  
<sup>476</sup> posed; as restated below:

- <sup>477</sup> 1. What is the geologic structure of the upper crust beneath the Ross Ice Shelf?  
<sup>478</sup> If there are sediments, what is their thickness and distribution? Where are  
<sup>479</sup> the major faults likely located?
- <sup>480</sup> 2. How can bathymetry beneath an ice shelf best be modelled? Are there further  
<sup>481</sup> improvements that can be made to the gravity-inversion process? What are  
<sup>482</sup> the predominant sources of uncertainty, and how can these be limited?

483     3. How deep is the bathymetry beneath the Ross Ice Shelf and where are we most  
484       and least certain about it?

485     4. What are the geologic controls on the Ross Ice Shelf's stability?

486       Here we draw from the various research chapters to provide answers to these  
487       questions.

## 488     5.1 Investigating geologic structures

### 489     Research question 1

490     To address research question 1 we sought to model the depth of the crystalline base-  
491       ment rock beneath the ice shelf. We accomplished this with a depth-to-magnetic  
492       source technique, which used airborne magnetic data and was calibrated to seismi-  
493       cally imaged basement depths of the Ross Sea. Our resulting basement topography  
494       revealed large-scale, fault-controlled extensional basins throughout the sub-Ross Ice  
495       Shelf crust (Figure 5.1f). Above this basement sits various sediments, likely rang-  
496       ing from coherent sedimentary rock to unconsolidated recent glacial and marine  
497       deposits. While there is a continuous drape of sediments across the entire ice shelf,  
498       we also image several distinct depocenters; the Western Ross Basin, covering the  
499       East Antarctic half of the ice shelf, and several basins on the West Antarctic side,  
500       including the Siple Dome Basin and the Crary Trough. These results were incor-  
501       porated into an Antarctic-wide review of sedimentary basins (Figure 5.1a Aitken  
502       et al., 2023a), showing the widespread distribution of similar basins across much of  
503       Antarctica. From our findings, we were able to draw a wide range of implications,  
504       ranging from tectonic influence on ice dynamics along the Siple Coast to the buried  
505       and subsided remnants of an above-sea-level Oligocene mountain range, which likely  
506       accommodated alpine glaciers. These results provided the first view of the upper  
507       crust beneath the entirety of the Ross Ice Shelf.

508

## 509     5.2 Developing a gravity inversion

### 510     Research question 2

511     To provide modellers with accurate bathymetry depths beneath the Ross Ice Shelf,  
512       we utilized a gravity inversion technique. While there is an existing gravity-inverted  
513       bathymetry model for the Ross Ice Shelf (Tinto et al., 2019), the reported uncer-  
514       tainties were spatially uniform. To properly address the uncertainties, we chose to  
515       develop a new gravity inversion algorithm. In addition, since the majority of gravity  
516       inversions use proprietary and expensive software, in an effort towards open-source  
517       and reproducible science, we chose to develop our gravity inversion using Python  
518       and release the code in an online repository.

519

520       Chapter 3 described this algorithm in detail. Extensive testing of various syn-  
521       thetic and semi-realistic datasets revealed several intricacies of performing a gravity  
522       inversion to attain a bathymetry model. The estimation and removal of the regional  
523       component of gravity, which occurs in the data reduction steps before the inversion,  
524       accounts for the majority of the error in the model. There are various techniques to

remove the regional field. We explore several of these methods and provide recommendations to best reduce the errors. Our uncertainty analysis highlighted regions of either steep topography or high gradient gravity anomalies as key regions where additional bathymetry measurements will make a significant contribution to reducing uncertainties. These suggestions of where to collect additional data should be considered alongside key regions of investigation identified through ocean modelling. Our findings suggest the quantity of bathymetry measurements is more important for reducing inversion uncertainty than the quality of these measurements. Conversely, we show an increased sensitivity of the inversion results to the noise in the gravity data, relative to the density of gravity data collected. This suggests optimizing quantity over quality for bathymetry constraints while optimizing quality over quantity for gravity observation data. We hope these suggestions are able to better inform future Antarctic data collection for the goal of improving sub-ice shelf bathymetry models.

As part of Chapter 4, we compared our methods, of both the gravity reduction process and the inversion procedure, to all past bathymetry models conducted in Antarctica, as well as several from Greenland. Several other inversions have used a regional separation method similar to ours, however, none of these have provided an assessment of the associated uncertainties related to this method, which we found to be significant. We also found that all other inversions utilized a non-rigorous method of correcting the gravity data for the effects of ice, water, and topography. While the error introduced is likely small, with modern computing, applying this correction correctly is trivial.

From the other studies, excluding those with undocumented inversion algorithms, we found only one study which used a conventional regularized least-squares approach, similar to ours. Comparing our uncertainty analysis to past inversions revealed only two studies that report spatially variable uncertainties of their bathymetry model. It is our hope that the improvements made for the gravity inversion process are incorporated in future inversion in order to attain better estimates of uncertainties.

557

## 558 5.3 Modelling Ross Ice Shelf Bathymetry

### 559 Research question 3

With the gravity inversion methodology laid out in Chapter 3, we created a new model of sub-Ross Ice Shelf bathymetry (Figure 5.1e). This model highlighted some important differences from past bathymetry models. In general, our model has more varied topography, compared to the smooth Bedmap2 model, and the intermediate BedMachine model. Compared to Bedmap2, we report significantly deeper bathymetry along the entirety of the grounding zone, including notably deeper areas near the Kamb Ice Stream, along the west side of Roosevelt Island, and south of Minna Bluff. Compared to the past inverted bathymetry (Tinto et al., 2019), our results are deeper along the Siple Coast but vary between deeper and shallower along the Transantarctic Mountain front. Our uncertainty analysis identified gravity data as the largest component of the overall uncertainty, while the distance from

the nearest constraint and interpolation parameter values contributed significantly to the spatial variability of the uncertainty. From this, the largest uncertainties were found either far from constraints, or along the steep topography of the Transantarctic Mountains. This highlighted several locations where future seismic surveys would be able to effectively reduce uncertainties.

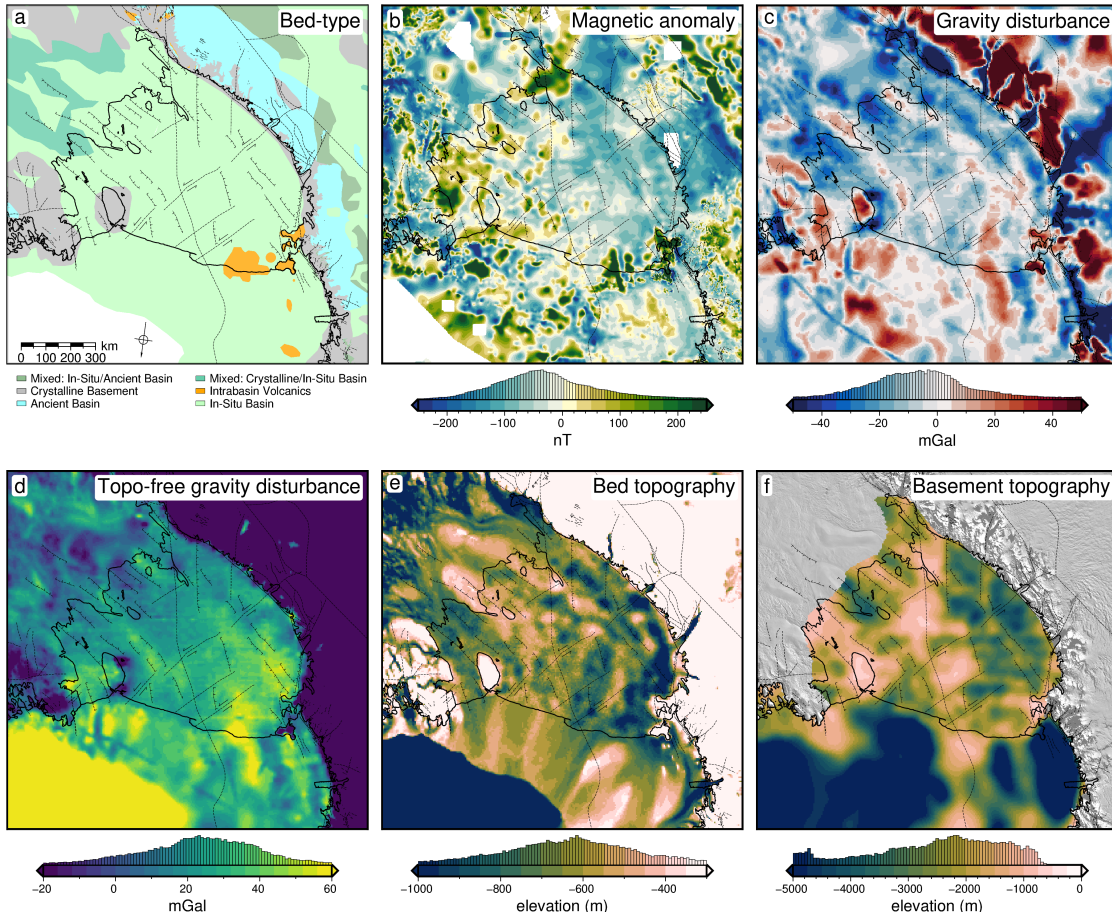


**Figure 5.1:** Summary of southern Ross Embayment geophysical and geologic information. **a)** Generalized geologic classification of the bed from Aitken et al. (2023b), **b)** ROSETTA-Ice airborne magnetic anomalies (Tinto et al., 2019) merged with ADMAP2 magnetic anomaly compilation (Golynsky et al., 2018), **c)** Gravity disturbance compilation from Forsberg (2020), include ROSETTA-Ice data. **d)** Topo-free gravity disturbance (Complete Bouguer disturbance) after a terrain mass effect correction was applied to **c**, using ice surface and ice base from BedMachine v3 Morlighem (2022), and the gravity-inverted bathymetry. **e)** Inverted bathymetry from Chapter 4, **f)** Basement topography from Chapter 2. Solid black line shows the grounding line and ice front from Mouginot et al. (2017). Fainter black lines show inferred (dashed) and exposed (solid) faults from a combination of Chapter 2 and Cox et al. (2023). Background imagery in **f** from MODIS-MOA (Scambos et al., 2007).

## 5.4 Geologic controls on Ross Ice Shelf Stability

### Research question 4

Next, we synthesize our findings which relate to the geologic influence on the Ross Ice Shelf, in an attempt to answer research question 4. We start with the controls on the ice shelf as it is today, before speculating on what these geologic controls were in the past or will be in the future.

**582 5.4.1 Present controls****583 Basal melt**

584 Basal mass loss of the Ross Ice Shelf is dominated at the deep grounding zones,  
585 where relatively cool High Salinity Shelf Water is able to induce melting due to the  
586 high pressure at depth (Tinto et al., 2019; Adusumilli et al., 2020). These inflows of  
587 cold and dense water occur along the seafloor and are guided south beneath the ice  
588 shelf by bathymetric features (Holland, 2008). Our bathymetry model (Figure 5.1e)  
589 shows a deep trough ranging from the western ice front, past Minna Bluff, along  
590 the grounding line, ending near Nimrod Glacier. This trough is deeper than both  
591 past bathymetry models, further supporting the Transantarctic Mountain front as  
592 a location with a strong susceptibility to basal melt. At the Nimrod Glacier outlet,  
593 this trough steps to the east by ~ 100km, and eventually ends along the south flank  
594 of Crary Ice Rise. This continuous trough from the ice front near Ross Island to the  
595 grounding zone at Crary Ice Rise is not apparent in past models. This may provide  
596 an avenue for High Salinity Shelf Water to reach the Siple Coast; a scenario which  
597 should be further explored.

598

599 The Hayes Bank, to the west of Roosevelt Island, has been identified as the pri-  
600 mary location of inflow of warm Circumpolar Deep Water (Tinto et al., 2019; Das  
601 et al., 2020). We model a region of deeper-than-previous seen bathymetry along  
602 the west edge of Roosevelt Island and propose this as a location that may allow the  
603 incursion of this ocean water with a high potential for melt. Additionally, along the  
604 Shirase Coast, south of Roosevelt Island, we model a thicker ocean cavity than past  
605 estimates. This may allow further penetration of water which enters the shelf near  
606 Hayes Bank.

607

**608 5.4.1.1 Modern pinning points**

609 Analysis of Ross Ice Shelf's pinning points has shown that the effective resistance as  
610 well as the temporal persistence of pinning points are not tied solely to their size, but  
611 are strongly influenced by the competency of the bedrock (Still et al., 2019; Still &  
612 Hulbe, 2021). A really small pinning points which exert large effective resistance are  
613 assumed to be grounded on bed with a high friction coefficient, while large pinning  
614 points which exert only minor resistance are assumed to be grounded on an easily  
615 deformable substrate. Based on the ratio of area to effective resistance, Still et al.  
616 (2019) suggested the bed beneath the Shirase Coast Ice Ripples, to the south-east  
617 of Roosevelt Island (Figure 5.2), is likely composed of competent bedrock with a  
618 high friction coefficient. Conversely, they suggest pinning point #14, just north of  
619 Crary Ice Rise, to be grounded on easily deformable till. The downstream extent  
620 of streaklines from pinning points provides an estimate of the temporal persistence  
621 of these features. Based on these streaklines, the Shirase Coast Ice Ripples and  
622 the Crary Ice Rise have likely been grounded for hundreds of years, while the large  
623 Steershead Ice Rise, just west of Siple Dome, only became grounded within the last  
624 400 years (Still et al., 2019; Fahnestock et al., 2000).

625

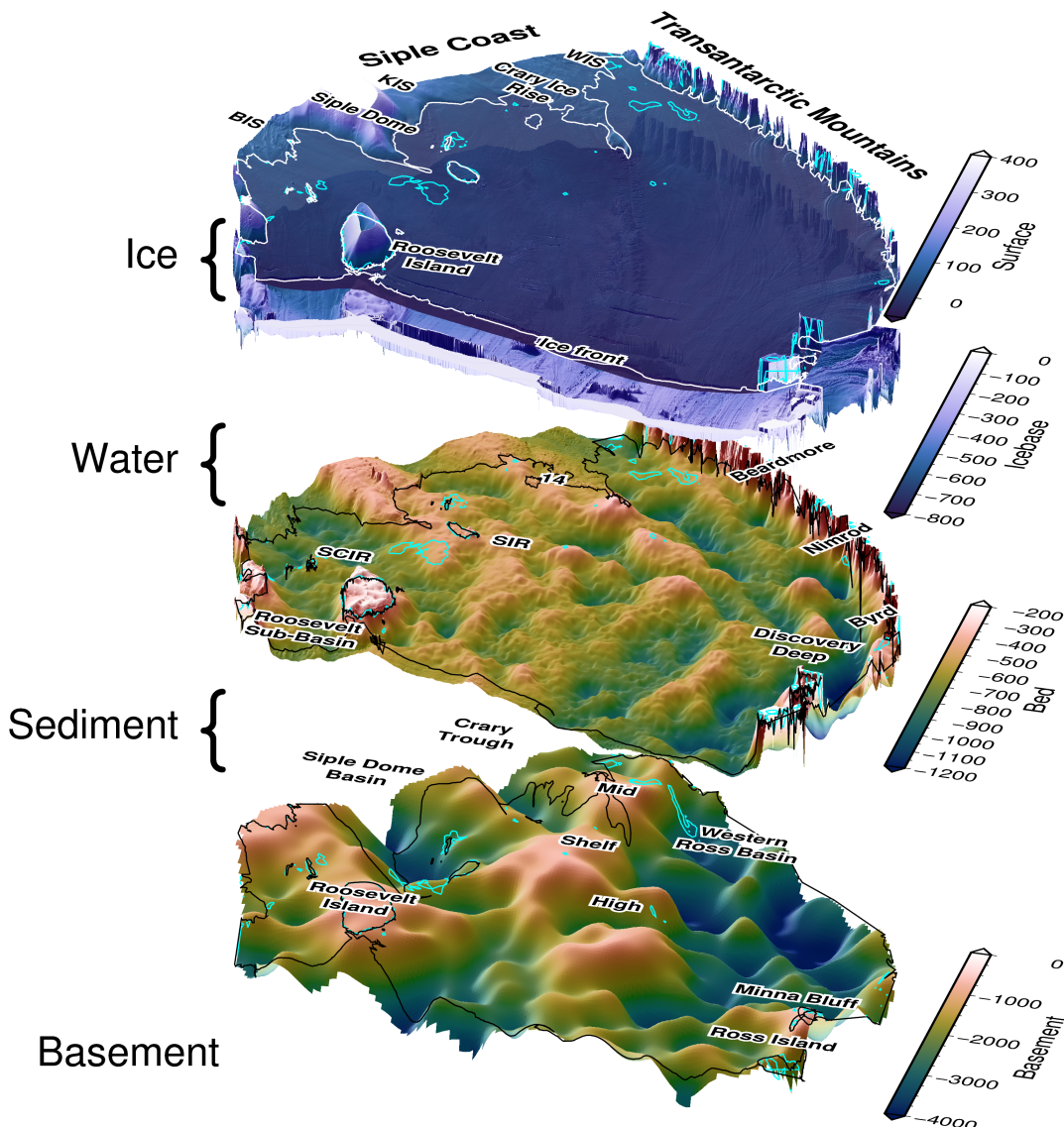


**Figure 5.2:** A 3D perspective view of the structure of the Ross Ice Shelf. Starting at the top, ice surface, and ice base from BedMachine v3 (Morlighem, 2022; Morlighem et al., 2020), inverted bathymetry results from Chapter 4, and basement topography from Chapter 2. Grounding line shown in all layers if from Morlighem (2022). Bright blue contour shows 20 m water column thickness. Note each layer has an independent vertical exaggeration to aid in visualization.

## 626 Persistent pinning points

627 Our basement and sediment thickness results provide support for many of these  
 628 observations of ice dynamics. The Shirase Coast Ice Ripples, predicted to have  
 629 been long-lasting and grounded on competent bedrock, are shown in our basement  
 630 results to sit upon a large basement high, with thin sedimentary cover. This implies  
 631 both that the bedrock beneath the pinning point is either crystalline basement, or  
 632 very coarse sediment from minimally re-worked basement material, and that the  
 633 elevation of the bed is stable. This stability is likely due to both the tectonic nature  
 634 of the bed as a fault-bound horst, and the higher strength of the bedrock, able to  
 635 resist erosion by the overriding ice. Similarly, the persistence of Crary Ice Rise in  
 636 the glaciologic record may be owed to its location above a basement ridge. Of the

637 areas of possible recent grounding we identified, the region to the south of Crary Ice  
638 Rise, and the smaller area  $\sim$  200 km north of Crary Ice Rise, both are located on  
639 similar large basement highs with thin sedimentary cover. When grounded, these  
640 past pinning points likely imparted a large effective resistance on the overriding ice.  
641

## 642 Recent pinning points

643 The predicted deformable substrate of both Steershead Ice Rise and pinning point  
644 #14 (Still et al., 2019), as well as the recent grounding of Steershead Ice Rise  
645 (Fahnestock et al., 2000), are supported by our observations of these features being  
646 located over thick fault-bound sedimentary basins. These thick sediments provide  
647 material that is easily weathered into glacial till by the overriding ice, which lowers  
648 the effective resistance of the pinning point. If the basin bounding faults we predicted  
649 in Chapter 2 are truly active, they could accommodate local vertical bed movements  
650 associated with glacial isostatic adjustment following changing ice loads (Peltier et  
651 al., 2022; Steffen et al., 2021). For the very low-viscosity upper mantle and thin  
652 lithosphere beneath West Antarctica (Pappa et al., 2019; Chen et al., 2018), these  
653 solid earth responses to changing ice thickness may occur on decadal timescales  
654 (Barletta et al., 2018). This may help explain the short-lived history of these pinning  
655 points. One of the possible recent pinning points we identified is within the same  
656 sedimentary basin as Steershead Ice Rise (between Steershead Ice Rise and Roosevelt  
657 Island), and when grounded, likely shared these qualities. With these observations,  
658 we support the notion of a strong geologic control on the buttressing ability and  
659 persistence of pinning points throughout the Ross Ice Shelf. As the West Antarctic  
660 Ice Sheet thins, swift glacial isostatic rebound may lead to re-grounding; a response  
661 which may promote stability of the ice sheet (Coulon et al., 2021; Barletta et al.,  
662 2018; Kachuck et al., 2020). Accurate bathymetry beneath the Ross Ice Shelf is  
663 vital for knowing where this re-grounding may occur, and thus where new pinning  
664 points will develop.

### 665 5.4.1.2 Sediment distribution

666 The dynamics of Siple Coast ice streams are intrinsically tied to the bed which  
667 they flow over. The presence of sediments and sedimentary basins allows for several  
668 mechanisms to achieve the fast flow seen in these ice streams. 1) The sediments are  
669 able to deform in response to the shear stress of the overriding ice, allowing faster  
670 flow (Alley et al., 1986), 2) groundwater stored within the sedimentary basins both  
671 lubricates the ice base, reducing basal friction and increases till deformation, through  
672 increased pore-fluid pressure (Tulaczyk et al., 2000). Our results of Chapter 2 show  
673 a continuous drape of sediments across the ice shelf including along the Siple Coast  
674 grounding zone. The presence of these sediments helps explain the fast-flowing ice  
675 along this region. Additionally, we image several large sediment basins beneath the  
676 Siple Coast. The groundwater storage capabilities of such basins could provide up to  
677 half of the groundwater in the subglacial system of West Antarctica (Christoffersen  
678 et al., 2014). The southernmost of these sedimentary basins has been confirmed by a  
679 recent magnetotelluric survey, which identified  $> 1$  km of sediments with extensive  
680 groundwater storage (Gustafson et al., 2022). The other two basins we imaged,  
681 the Siple Dome Basin, and the Crary Trough (Figure 5.2), could be key drivers on  
682 subglacial hydrology beneath the Siple Coast.

**683 5.4.1.3 Geothermal heat flux at Siple Coast**

684 The last main geologic control on Ross Ice Shelf stability we propose is the distribution  
685 of geothermal heat along the Siple Coast. Geothermal heat flux is one of the least constrained boundary conditions for Antarctica (Pollard et al., 2005; Larour  
686 et al., 2012; Seroussi et al., 2017). High geothermal heat supplied to the ice base  
687 can accelerate flow by 1) increasing englacial temperatures, reducing ice viscosity,  
688 2) increasing basal lubrication through meltwater production and 3) increasing the  
689 ability of subglacial till to deform, through water-saturation (Pollard et al., 2005;  
690 Golledge et al., 2014). While we don't provide any direct measurements of geothermal  
691 heat flux, our fault-bound sedimentary basins along the Siple Coast provide  
692 important insights into the temporal and spatial variability expected for geothermal  
693 heat flux along the Siple Coast.

694

**696 Spatial control on geothermal heat**

697 Measurements and predictions of geothermal heat flux along the Siple Coast are  
698 shown to vary significantly, even between nearby (within  $\sim 100$  km) measurements  
699 (Begeman et al., 2017; Fox Maule et al., 2005). This high spatial variability is  
700 attributed to the localization of heat due to upper crustal structures (Begeman et  
701 al., 2017). Faults and basement margins act as efficient fluid conduits, which can  
702 localize the already regionally elevated heat (e.g., Fox Maule et al., 2005; Burton-  
703 Johnson et al., 2020), resulting in vastly enhanced heat flow to the ice base (Gooch  
704 et al., 2016), which is likely the cause of the anomalously high heat flow measured  
705 at Subglacial Lake Whillans ( $285 \text{ mW/m}^2$ , Fisher et al., 2015). We hypothesized in  
706 Chapter 2 that these faults not only provide a spatial control on geothermal heat  
707 flux, but a temporal control as well.

708

**709 Temporal control on geothermal heat**

710 As ice thickness has varied throughout the Holocene, the changing ice overburden  
711 pressure on the subglacial sediments drives the discharge and recharge of these sedi-  
712 mentary aquifers (Gooch et al., 2016; Li et al., 2022). This fluid movement is  
713 accommodated along fault-damage zones and impermeable basement margins (Jolie  
714 et al., 2021). This may present a positive feedback, where thickening ice drives  
715 groundwater into the aquifers, advecting heat away from the ice base, which slows  
716 the flow of ice, leading to increased thickness. Similarly, as ice thins, the reduced  
717 overburden on the aquifers results in water discharge to the ice base and an associ-  
718 ated localization of heat. The resulting increased flow speed and thinning of the ice  
719 further reduces the overburden pressure. This time-variable influence of faults and  
720 sedimentary basins on the overriding ice requires further consideration but is likely  
721 an influential component of these complex interactions between the solid earth and  
722 ice at the Siple Coast. We now discuss various implications of our geologic findings  
723 for understanding past and future ice dynamics of the Ross Ice Shelf region.

724

### 5.4.2 Constraining past and future ice sheet behaviour

While all of the above geologic controls on the ice sheet likely existed in the past and will continue into the future, our study has several implications that are exclusive to past or future ice sheet configurations. The pinning points we discussed, and the regions of thin draft, were all likely pinning points during periods of thicker ice. Since the Last Glacial Maximum (~ 22 kya) retreat of the grounding line from the outer shelf edge has been primarily controlled by the physiography of the bed, as well as its geologic composition (Halberstadt et al., 2016; Anderson et al., 2019). While the retreat dynamics have been well studied in the Ross Sea, where the open ocean conditions allow seismic and high-resolution multi-beam sonar surveying (Halberstadt et al., 2016; Anderson et al., 2019), and drill cores provide sedimentary records (McKay et al., 2016), under the Ross Ice Shelf there has been very little investigation on retreat dynamics, apart from modelling studies (Lowry et al., 2020; Kingslake et al., 2018). Here we have provided the physiography of the region, through the sub-Ross Ice Shelf bathymetry model, which should give insights into the retreat dynamics throughout the Holocene. Understanding the way in which the Ross Ice Shelf and paleo Ross Ice Sheet responded during past periods of warming is vital to predicting its future response to a warming climate.

743

### Retreat dynamics

While we don't provide any estimate of the age of the sea floor sediments, the general physiography of the sea floor can provide some insights. The eastern side of the ice shelf, apart from Roosevelt Island, shows similar physiography to the eastern Ross Sea, with relatively flat bathymetry without major banks or troughs. There, the subdued bathymetry resulted in a stepwise style of grounding line retreat throughout the Miocene, with the stabilizing build-up of grounding zone wedges, followed by decoupling and rapid retreat of 10's of kilometres (Anderson et al., 2019; Bart et al., 2017). The bathymetry of the western Ross Ice Shelf, characterized by depth troughs and shallow banks, is similar to that of the western Ross Sea. There, the retreat style, also controlled by the bathymetry, was continuous and complex, as ice streams followed the bathymetry in a continuous retreat back to the outlet valleys in the Transantarctic Mountains (Halberstadt et al., 2016; Anderson et al., 2019). Retreat style and physiography are interdependent; smooth topography leads to wide ice streams, which when retreating in a stepwise fashion, stagnate and deposit significant sediment volume, adding to the smooth nature of the topography. Conversely, steep topography confines flowing ice, leading to narrow ice streams. These are thought to retreat in a continuous fashion, where a lack of stagnation leads to minimal grounding zone deposition. Over repeated cycles of advance and retreat, this leads to the scouring of sediments from the inner shelf, and an over-deepened, landward sloping inner shelf (Anderson et al., 2019). These contrasting styles of retreat proposed for the eastern and western Ross Ice Shelf may be in part responsible for the varied bathymetry found on either side of the ice shelf. The above section discussed our bathymetry results in relation to past and future ice dynamics. Next, we discuss the implication of our basement topography on the glacial history of the region.

770

**771 Glacial initialization**

772 During the Oligocene, the Ross Embayment contained a long and broad moun-  
773 tain range emergent above sea level, trending N-S from the Ross Sea through the  
774 ice shelf. This feature was first recognized from the drill cores of DSDP (Deep  
775 Sea Drilling Project) site 270 in the Ross Sea (Figure ???, Leckie, 1983), where a  
776 420 m sedimentary sequence with depositional environments ranging from above  
777 sea level to  $\sim$  500 below sea level was found, dating from late Oligocene to early  
778 Miocene (Kulhanek et al., 2019). Beneath this sequence was crystalline basement.  
779 The broad dome-like shape of this basement high was revealed by shipborne seis-  
780 mic surveys (Brancolini et al., 1995), which imaged a similar basement high further  
781 north. These basement features were termed the Northern and Southern Central  
782 High. Seismic data also revealed small U-shaped channels within the acoustic base-  
783 ment, which were attributed to alpine glaciation (De Santis et al., 1995). Off the  
784 flanks of these fault-bound basement highs, wider troughs in the basement were im-  
785 aged and attributed to the erosion of ice streams flowing off these basement highs.  
786 During the late Oligocene, ice caps nucleated on these subaerial basement features  
787 (De Santis et al., 1995). Thermal subsidence following the onset of mid-Cretaceous  
788 West Antarctic Rift System extension (Karner et al., 2005; Wilson & Luyendyk,  
789 2009) gradually submerged these basement highs (De Santis, 1999). In addition  
790 to the North and South Central High features in the Ross Sea, paleotopographic  
791 reconstructions of the Oligocene (Paxman et al., 2019; Wilson et al., 2012) have  
792 predicted the continuation of this broad subaerial mountain range under the Ross  
793 Ice Shelf. Our depth to magnetic basement (Chapter 2) provided the first observa-  
794 tions of the feature beneath the Ross Ice Shelf, which we termed the Mid Shelf High.

795

796 The strong continuity of the Mid Shelf High with the Ross Sea's Central High  
797 suggests that these features have similar histories. We propose the three blocks of  
798 the Mid Shelf High were emergent and hosted ice caps in the Oligocene. Following  
799 their submersion, likely in the early to middle Miocene (De Santis, 1999) these  
800 features would have acted as major bathymetry pinning points, similar to the modern  
801 Roosevelt Island. We suggest this chain of shallow basement blocks formed a long-  
802 lasting catchment divide of both sediment transport and ice flow between East and  
803 West Antarctica. This divide has been predicted as far back as the Paleogene, from  
804 distinct microfossil assemblages on either side of the Ross Embayment (Coenen et  
805 al., 2019). Since the Last Glacial Maximum, the Central High has been thought to  
806 be an ice flow divide, separating ice originating from the East and West Antarctic  
807 Ice Sheets (Li et al., 2020; Licht et al., 2014; Licht et al., 2005). The prominent Mid  
808 Shelf High / Central High appears to have played a central role in the history of the  
809 Ross Embayment since the Oligocene.

**810 5.5 Future work**

811 Here we provide several suggestions for future research and fieldwork related to  
812 this thesis. A primary piece of future work resulting from this thesis should be  
813 the incorporation of the updated bathymetry into a sub-ice shelf circulation model.  
814 Ideally, this would incorporate the spatially variable uncertainty of the bathymetry.  
815 To better improve the bathymetry model and reduce uncertainties, we suggest three  
816 alternatives for field seasons on the Ross Ice Shelf.

- 817 1. Collect additional seismic depth measurements along the Transantarctic Mountain front. This would serve to lower uncertainties in the bathymetry associated  
818 with the nearby steep topography. A traverse-style field season would be best for this to accommodate the linear nature of the grounding zone. Collecting  
819 occasional cross lines, running perpendicular to the grounding line, would likely image the range front faults, commonly inferred by only rarely imaged.  
820
- 821
- 822
- 823 2. A seismic survey of the central block of the Mid Shelf High. This survey would accomplish three goals. First, it would fill one of the two major gaps  
824 in bathymetry measurements in the central ice shelf, reducing the bathymetry uncertainty. Secondly, it would inform on the nature of the Mid Shelf High as  
825 a past pinning point and nucleation site of Oligocene ice caps. Lastly, it would act as a site survey for potential sediment drilling. The thin sedimentary  
826 cover of the Mid Shelf High may provide a good target for future drilling since a temporally wide-ranging sequence may be concentrated into a thin  
827 sedimentary package.  
828
- 829
- 830
- 831
- 832 3. Conduct a regional seismic survey across portions of the Siple Coast to better image the sedimentary basins and basin bounding faults, especially where the  
833 fault proposed in Chapter 2 may interact with the ice streams.  
834

835 Based on our comprehensive review of past Antarctic bathymetry gravity inv-  
836 ersions, we make several suggestions for future inversions. To test the inversion  
837 method developed here, it would be useful to perform another inversion for an ice  
838 shelf that has been previously inverted. The three best options for this would be the  
839 Getz Ice Shelf, the Thwaites Glacier, and the Pine Island Glacier. The bathymetry  
840 beneath each of these ice shelves has been inverted three separate times, allowing the  
841 comparison of several different methods. The Getz Ice shelf bathymetry has been  
842 inverted in 2D (Wei et al., 2020; Cochran et al., 2020), and with a 3D frequency-  
843 based inversion (Millan et al., 2020). The Thwaites cavity has also been inverted  
844 in both 2D (Tinto & Bell, 2011) and 3D, with both the "topo-shift method" (Jor-  
845 dan et al., 2020), and a frequency-based method (Millan et al., 2017). Lastly, the  
846 Pine Island Glacier bathymetry has been inversion twice with Simulated Annealing  
847 (Muto et al., 2016; Muto et al., 2013b), and once with a frequency-based inversion  
848 (Millan et al., 2017). To compare to a wider range of methods, the Thwaites glacier  
849 would be optimal. To gain insights into the effectiveness of our uncertainty analysis,  
850 Pine Island Glacier should be chosen since spatially variable uncertainty estimates  
851 exist from the studies which used Simulated Annealing.

852 Of the major Antarctic ice shelves, there are four that stand out as prime can-  
853 didates for a future inversion if the goal is to increase our sub-ice shelf bathymetric  
854 knowledge. These include the Larsen C Ice Shelf, the Ronne Filchner Ice Shelf, the  
855 Riiser-Larsen Ice Shelf, and the Shackleton Ice Shelf.

- 856
- 857 1. Larsen C is the largest ice shelf on the Antarctic Peninsula, yet bathymetry  
858 knowledge beneath it is still limited. A bathymetry inversion has been con-  
859 ducted (Cochran & Bell, 2012), but comparison with seismic constraints re-  
860 vealed large uncertainties in the model. A recent constraint compilation and  
861 new seismic data (Brisbourne et al., 2020) make this an ideal candidate with-  
862 out needing any field work. Additional gravity data has also been collected

863 over the ice shelf during 2016, 2017, and 2018 Operation Ice Bridge flights  
864 (“IceBridge Sander AIRGrav L1B Geolocated Free Air Gravity Anomalies,  
865 Version 1”, 2020).

- 866 2. The Ronne Filchner is the second-largest ice shelf, yet has not been included  
867 in a gravity inversion. An extensive array of seismic constraints, similar to the  
868 RIGGS survey of the Ross Ice Shelf exists (Fretwell et al., 2013; Rosier et al.,  
869 2018), and gravity data from compiled from Russian airborne and ground-  
870 based surveys (Aleshkova et al., 2000; Studinger & Miller, 1999) is accessible  
871 as part of the continent-wide AntGG gravity compilation (Scheinert et al.,  
872 2016).
- 873 3. and 4. The Riiser-Larsen and the Shackleton Ice Shelves are the 5th and 7th  
874 largest ice shelves, respectively. To our knowledge, there is no bathymetry  
875 knowledge beneath the entirety of either shelf. Gravity data exists for both  
876 shelves from the AntGG compilation (Scheinert et al., 2016). Performing  
877 inversions for these shelves would require extensive seismic data acquisition to  
878 be adequately constrained.

879 Lastly, we highlight a few alternative use cases and limitations for our gravity  
880 inversion algorithm. While this has been developed for a regional-scale sub-ice shelf  
881 application, at its core the inversion is a standard geometric (sometimes referred  
882 to as structural) inversion. Therefore, this code can be used to invert any topo-  
883 graphic surface of a user-defined density contrast based on input gravity anomaly  
884 data. It is compatible with domains ranging from small-scale, local areas, to large  
885 domains such as ours ( $1000 \times 1000$  km). However, domains significantly larger  
886 than ours (continental scale) will introduce inaccuracies due to our use of vertical  
887 right-rectangular prisms, which makes assumptions of a planar Earth. For these  
888 continental to global scale inversions, vertical prisms should be replaced with spher-  
889 ical prisms (tesseroids), as implemented by (Uieda & Barbosa, 2017). With this, our  
890 inversion will work for other applications, such as predicting regional Moho depths,  
891 the sediment-basement contact, or determining bed depths beneath grounded ice,  
892 under subglacial lakes, or in the open ocean. We hope this code is used by others  
893 for these various applications.

## 894 5.6 Concluding remark

895 The primary aim of this thesis was to use existing airborne geophysical data to better  
896 characterize the geology and physiography beneath Antarctica’s Ross Ice Shelf. We  
897 used and developed several geophysical techniques to accomplish this. We first used  
898 variations in Earth’s magnetic field measured over the ice shelf to model the spatial  
899 distribution and thickness of sediments beneath the ice shelf. We then developed  
900 and extensively tested a geophysical inversion, which uses measurements of Earth’s  
901 gravity field to model the depth to the seafloor. With this, we created an updated  
902 model of the bathymetry beneath the ice shelf.

903  
904 From this geophysically informed knowledge of the upper crust of the sub-Ross  
905 Ice Shelf, we were able to draw inferences on the complex interactions between the  
906 solid Earth, ocean, and ice for the Ross Embayment. We highlighted the Siple  
907 Coast as a location with strong geologic control on ice dynamics, through 1) the

908 distribution of sediments, which control the competency of bedrock material beneath  
909 grounded ice, and 2) the location of deep sedimentary basins, which likely supply  
910 the ice base with lubricating water and localize the geothermal heat delivered to the  
911 ice. Our bathymetry model confirms the findings of past models which show a deep  
912 trough spanning from the ice front near Ross Island south along the Transantarctic  
913 Mountain Front. This trough likely guides High Salinity Shelf Water from the ice  
914 front to the deep grounding zone of the Transantarctic Mountain outlet glaciers,  
915 where it induces significant basal melting. Our spatial uncertainty results highlight  
916 the Transantarctic Mountain Front as the least-certain portion of the sub-ice shelf  
917 bathymetry model. Combined with this region's importance for basal melt, we  
918 suggest future seismic surveys target the mountain front. This thesis provides the  
919 necessary boundary conditions and estimates of their uncertainties for ice and ocean  
920 modellers to better characterize the Ross Ice Shelf's response to past, present, and  
921 future changes in the climate.